P4.1

Structure of the marine boundary layer during episodes of strong southerly winds along the coast of central Chile

Ricardo C. Muñoz*, René D. Garreaud

Departamento de Geofísica
Universidad de Chile
Santiago, Chile

1. Introduction

A low-level summertime jet along the western coast of the U.S. has been documented in the literature through several observational (Pomeroy and Parish (2001),Parish (2000), Bridger *et al.* (1993)) and modeling (Holt (1996),Burk and Thompson (1996),Cui *et al.* (1998),Bielli *et al.* (2002)) studies. Along the western coast of subtropical South America there exists also a similar jet, which we describe here based on Quikscat (QS) Version 3 data (Pickett *et al.*, 2003), and results obtained with the PSU/NCAR Mesoscale model MM5 (Grell *et al.*, 1994). We present also the attendant structure of the marine boundary layer (MBL).

Figure 1 shows contours of QS wind speed and wind vectors averaged over the months November-January (NDJ) of years 2000-2003, for a strip along the coast of north-central Chile, between 19^o S and 43^o S. The main feature is the maximum in wind speed located between 25^o S and 40^o S, at about 200 km off the coast. The maximum is noticeable as well in individual QS fields, though its intensity and position varies considerably. The variability in the surface wind field is illustrated in Figure 2. Panel a shows the average difference between the PM and AM QS fields, and therefore represents the diurnal cycle in the surface winds. The amplitude of the diurnal cycle is larger along the northern coast of Chile, but it is remarkably small in the region of the jet. Panel b shows contours of standard deviation in wind speeds considering only PM QS fields for months NDJ. It represents, therefore, the synoptic variability, which attains a maximum in the coastal region close to the jet. In terms of seasonal variability (not shown) the jet shows a tendency to be located between 28 and 32 S between July-September and shift southwards up to 37 S during October-February (southern hemisphere warm season).

2. Model results

We have used the MM5 model to simulate the period 1-20 October 2000, in which special observations on a ship were available. Figure 3 compares surface wind speeds from the model and QS data. Panels a and b show the surface wind speeds over the ocean averaged for the period 5-13 October 2000. The model reproduces very well the horizontal structure of the wind field, specially the

* *Corresponding author address*: Ricardo C. Muñoz, Departamento de Geofísica, Universidad de Chile, Blanco Encalada 2002, Santiago, Chile. Email: rmunoz@dgf.uchile.cl

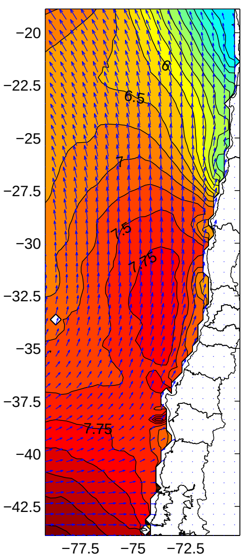

Fig. 1. Mean Quikscat-derived surface wind field for NDJ, 2000-2003 (contours in m/s).

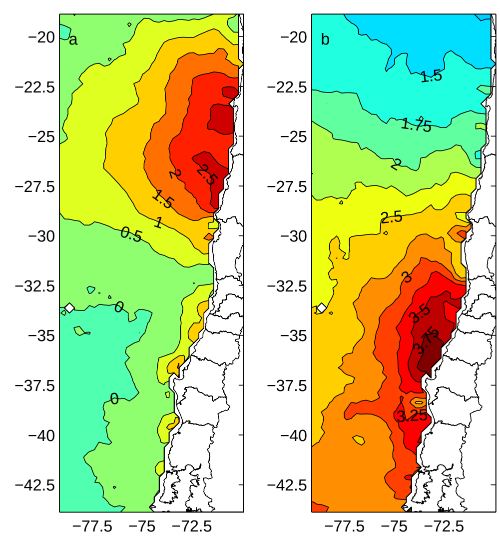

Fig. 2. a)Mean PM-AM wind speed field. b) Standard deviation of PM wind speed fields. Period considered is NDJ 2000-2003, all contours in m/s.

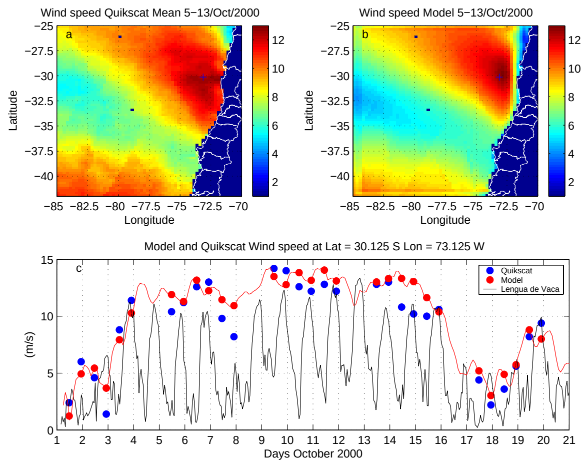

FIG. 3. Comparison of model results and observations. a) Average surface wind speed derived from QS for period 5-13 October 2000. b) Average first-layer wind speed from model output (color scales in m/s). c) Time series of wind speed for station Lengua de Vaca (30 S at the coast, fine line), for QS data at point 30.1 S, 73.1 W (closed blue circles), and for model output at same point (line with red circles).

maximum near the coast at 30 S. Panel c shows time series of surface wind speed for a point located in the region of maximum wind speeds. The closed circles in panel c are the 2-daily QS wind speed and the line with open circles are the model outputs for the same point. The model reproduces well the time variability of the wind speed at this location, which is characterized by a period of larger wind speeds between 4 -15 October 2000. In the data and the model the amplitude of the diurnal cycle in wind speed off the coast is small compared to the synoptic variability. The fine continuous line in panel c shows wind speed measured at the coastal station Lengua de Vaca (30 S). The diurnal cycle at this point is much larger than a few kilometers off the coast.

The occurrence of the jet is understood by using the model outputs to diagnose the terms in the momentum budget. In particular we compute averages for the period 9-11 October 2000, characterized by rather stationary conditions in the jet. The zonal momentum budget is very gesotrophic (not shown). The zonal wind speed, however, is very subgeostrophic, and therefore the meridional momentum balance is far from geostrophy. The main term in the meridional momentum balance is the pressure gradient (PG) term. Its averaged field at a height of 312 m above the sea is shown in Figure 4. The general synoptic pattern for this period shows higher pressures in the southern portion of the domain, which produces a positive PG tendency in V. Close to the coast, a mesoscale low pressure perturbation develops, that enhances the PG tendency to the south of the jet, and relaxes the PG to the north. The PG tendency is only partially balanced by Coriolis deflection of the zonal wind, while advection and friction play an equally important role in the balance (not shown).

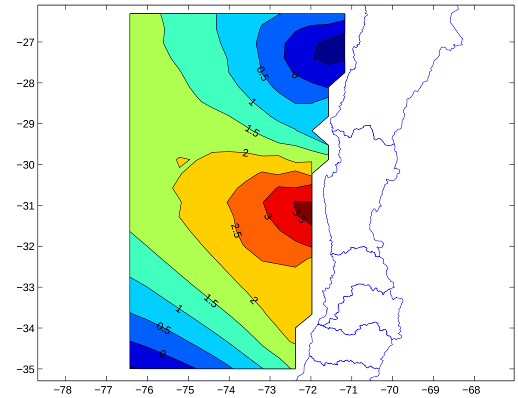

FIG. 4. Contours of pressure gradient tendency of meridional wind (m/s/hour) at 312 m above sea, averaged from model results for period 9-11 October 2000.

3. MBL STRUCTURE

Figures 5 and 6 show the meridional and zonal structure of V and temperature averaged for the period 9-11 October 2000. The locations of these cross sections coincide approximately with the meridional and zonal axes of the jet. The maximum meridional velocities occur close to the coast in the inversion layer capping the MBL. The latter increases in depth to the west. Special soundings available for the period show a similar slope of the MBL top, although the model MBL at the coast is shallower than in the observations (not shown). The meridional cross section of temperature (Figure 5 b) suggests the importance of the intense meridional wind in enhancing the stability at the top of the MBL. In the layer above the MBL there are strong horizontal gradients in temperature in both directions, with colder air to the west and south. Meridional cross sections of vertical velocities show mean positive values to the north of the jet and development of a stratus layer at the top of the MBL (not shown).

The depth of the MBL does not change significantly in the meridional direction. Figure 7a shows a meridional

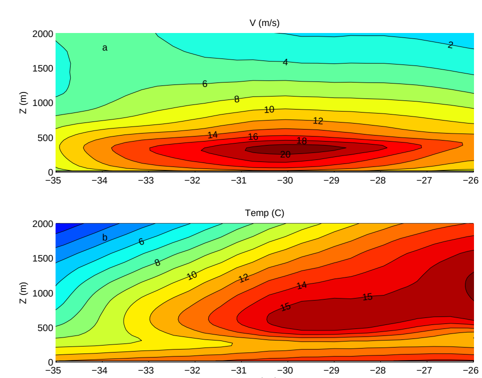

FIG. 5. Meridional-vertical cross sections at longitude 72.6 W averaged for period 9-11 October 2000. a) Meridional velocity (m/s), b) Temperature (C).

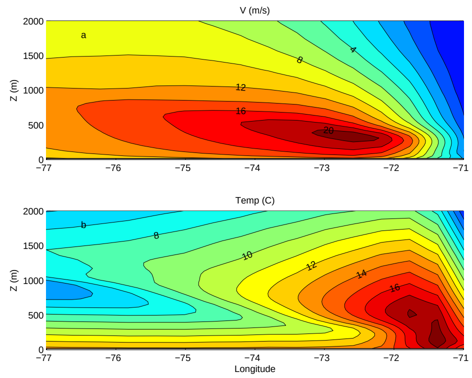

FIG. 6. Zonal-vertical cross sections at latitude 30 S averaged for period 9-11 October 2000. a) Meridional velocity (m/s), b) Temperature (C).

cross section of turbulent kinetic energy (TKE). Maximum values of TKE are located in the jet region. Panels b and c of the same figure show the shear production and buoyant production of TKE, respectively. The MBL in this case is dominated by shear production, whereas buoyant production is important as a sink of TKE in the inversion layer at the top of the MBL to the north of the jet.

4. Concluding remarks

Data and model results suggest that the diurnal cycle of the coastal jet off central Chile is small, while its synoptic variability is significant. The jet appears to be in a semigeostrophic balance. Zonally, the force balance is geostrophic, but in the meridional direction the pressure gradient is not balanced by Coriolis, but by a combination of advection and friction. The latter determines the position and intensity of the maximum in meridional wind speed. The turbulence in the marine boundary layer attendant to the jet is dominated by shear production. Although the depth of the MBL does not change much along the axis of the jet, the stability of the inversion capping the MBL is maximum in the region of the jet.

Acknowledgements.
This research was supported by FONDECYT (Chile) Grant 1020833.

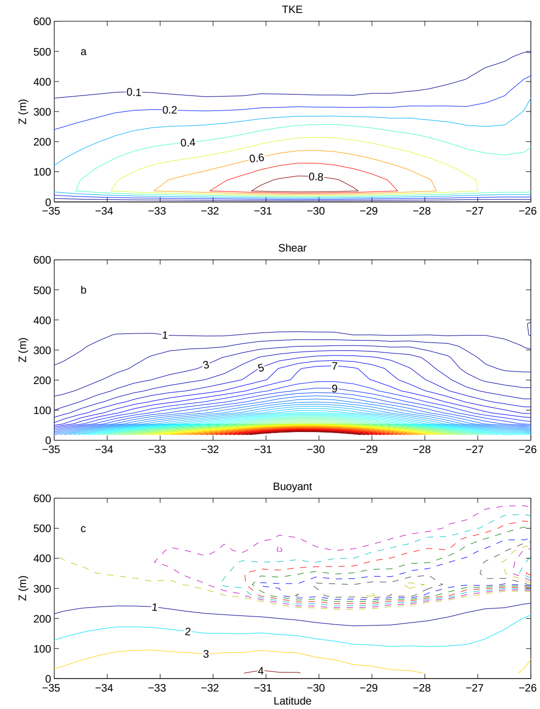

FIG. 7. Meridional-vertical cross sections at longitude 72.6 W averaged for period 9-11 October 2000. a) TKE (m2/s2), b) Shear production (m2/s2/hour), c) Buoyant production (m2/s2/hour) (dashed contours are negative values with -0.1 m2/s2/hour interval).

References

Bielli, S., P. Barbour, R. Samelson, E. Skyllingstad, and J. Wilczak, 2002: Numerical study of the diurnal cycle along the central Oregon coast during summertime northerly flow. *Mon. Wea. Rev.*, **130**, 992–1008.

Bridger, A. F. C., W. C. Brick, and P. F. Lester, 1993: The structure of the marine inversion layer off the central California coast: Mesoscale conditions. *Mon. Wea. Rev.*, **121**, 335–351.

Burk, S. D., and W. T. Thompson, 1996: The summertime low-level jet and marine boundary layer structure along the California coast. *Mon. Wea. Rev.*, **124**, 668–686.

Cui, Z., M. Tjernstrom, and B. Grisogono, 1998: Idealized simulations of atmospheric coastal flow along the central coast of California. *J. Appl. Meteor.*, **37**, 1332–1363.

Grell, G. A., J. Dudhia, and D. R. Stauffer, 1994: A description of the fifth-generation Penn State/NCAR mesoscale model (MM5). Technical Report NCAR/TN-398+STR, NCAR.

Holt, T. R., 1996: Mesoscale forcing of a boundary layer jet along the California coast. *J. Geophys. Res.*, **101**, 4235–4254.

Parish, T. R., 2000: Forcing of the summertime low-level jet along the California coast. *J. Appl. Meteor.*, **39**, 2421–2433.

Pickett, M. H., W. Tang, L. K. Rosenfeld, and C. H. Wash, 2003: QuikSCAT satellite comparisons with nearshore buoy wind data off the U.S. west coast. *J. Atmos. Oceanic Technol.*, **20**, 1869–1879.

Pomeroy, K. R., and T. R. Parish, 2001: A case study of the interaction of the summertime coastal jet with the California topography. *Mon. Wea. Rev.*, **129**, 530–539.